Available online at www.sciencedirect.com
ScienceDirect
Computer Coupling of Phase Diagrams and Thermochemistry 31 (2007) 468–478
www.elsevier.com/locate/calphad

The experimental study of the Bi–Sn, Bi–Zn and Bi–Sn–Zn systems

M.H. Braga[a,*], J. Vizdal[b,c], A. Kroupa[c], J. Ferreira[d], D. Soares[e], L.F. Malheiros[f]

[a] *GMM-IMAT, Department of Physics, FEUP, R. Dr. Roberto Frias s/n, 4200-465 Porto, Portugal*
[b] *Institute of Mat. Sci. and Eng., Faculty of Mechanical Engineering, Brno University of Technology, Technicka* 2896/2*, 616 69 Brno, Czech Republic*
[c] *Institute of Physics of Materials AS CR. Zizkova 22, 616 62 Brno, Czech Republic*
[d] *INETI Laboratory, R. da Amieira – P.O. Box 1089, 4466-956 S. Mamede de Infesta, Portugal*
[e] *Department of Mechanical Engineering, School of Engineering of UM, Campus de Azurém, 4800-058 Guimarães, Portugal*
[f] *GMM-IMAT, Department of Metallurgical and Materials Engineering, FEUP, R. Dr. Roberto Frias s/n, 4200-465 Porto, Portugal*

Received 19 April 2006; received in revised form 10 April 2007; accepted 12 April 2007
Available online 22 May 2007

Abstract

The binary Bi–Sn was studied by means of SEM (Scanning Electron Microscopy)/EDS (Energy-Dispersive solid state Spectrometry), DTA (Differential Thermal Analysis)/DSC (Differential Scanning Calorimetry) and RT-XRD (Room Temperature X-Ray Diffraction) in order to clarify discrepancies concerning the Bi reported solubility in (Sn). It was found that (Sn) dissolves approximately 10 wt% of Bi at the eutectic temperature.

The experimental effort for the Bi–Zn system was limited to the investigation of the discrepancies concerning the solubility limit of Zn in (Bi) and the solubility of Bi in (Zn). Results indicate that the solubility of both elements in the respective solid solution is approximately 0.3 wt% at 200 °C.

Three different features were studied within the Bi–Sn–Zn system. Although there are enough data to establish the liquid miscibility gap occurring in the phase diagram of binary Bi–Zn, no data could be found for the ternary. Samples belonging to the isopleths with w(Bi) ∼ 10% and w(Sn) ∼ 5%, 13% and 19% were measured by DTA/DSC. The aim was to characterize the miscibility gap in the liquid phase. Samples belonging to the isopleths with w(Sn) ∼ 40%, 58%, 77/81% and w(Zn) ∼ 12% were also measured by DTA/DSC to complement the study of Bi–Sn–Zn. Solubilities in the solid terminal solutions were determined by SEM/EDS. Samples were also analyzed by RT-XRD and HT-XRD (High Temperature X-Ray Diffraction) confirming the DTA/DSC results for solid state phase *equilibria*.

Keywords: Bi–Sn–Zn; Bi–Sn; DTA/DSC; SEM/EDS; (RT/HT)-XRD

1. Introduction

Health problems (especially neurological and birth malformations) may arise from an excess of lead in human bodies. The excess of lead is due to water contamination. Hence, lead was added to the list of apprehensions with the environment [1].

The objective of COST 531 action "*Lead-free Solder Materials*" [2] (European Cooperation in the field of Scientific and Technical Research) is the study of systems that may be used as lead-free solders. The selection of these systems is based on technical and health considerations. The crucial technical properties to be analyzed should be: melting point, wettability, surface tension, viscosity of the liquid alloys at different temperatures, oxidation behavior, thermomechanical fatigue, etc.

The evaluation of experimental phase diagrams, measurement of the thermodynamic properties and consequent optimization of the corresponding phase diagrams (using the CALPHAD method) are some of the aims of the COST 531 action. The work presented here is a part of this effort.

Bi–Sn–Zn is one of the important systems studied in scope of the above mentioned program. For this system there were no data concerning the liquidus surface in the miscibility gap region (corresponding to the phase boundary Liquid/L1 + L2). A work from Muzaffar [3], concluded in 1923, includes only temperature data for the surface corresponding to the phase boundary Liquid + L1/Liquid + (Zn).

The solvus surfaces for (Bi) and (Sn) were also uncertain. These doubts concern mainly the Sn-rich region within the

* Corresponding author.
E-mail address: mbraga@fe.up.pt (M.H. Braga).

0364-5916/$ - see front matter © 2007 Elsevier Ltd. All rights reserved.
doi:10.1016/j.calphad.2007.04.004

Bi–Sn binary system. Nagasaki and Fujita [4] experimentally defined a (Sn) solvus curve that was not in good agreement with that from Oelsen and Golücke [5]. Experimental results from Ohtani and Ishida [6] were also in contradiction with those from [4]. Nevertheless, Ohtani and Ishida [6] (contradicting their own experimental results) and Lee et al. [7] used only the experimental data from Nagasaki and Fujita [4] in their thermodynamic assessment.

Concerning Bi–Zn, there was a significant discrepancy between the (Bi) solvus estimated by Massalski [8] and that calculated by Malakhov [9] (few wt% of Zn). Thus, targeted experimental alloys were prepared to determine the solubility of Zn in (Bi).

With the aim of clarifying the above indicated aspects of the binaries and ternary, almost all of the samples were studied by SEM/EDS/WDS (Wavelength-Dispersive crystal Spectrometer), RT-XRD/HT-XRD and by DTA/DSC.

2. Experimental

The Bi–Sn and Bi–Sn–Zn systems were objects of two different studies. One more devoted to phase transitions as well as to temperature measurements and the other to the equilibrium study. Hence, the experimental details were different according to the objective of the study and therefore will be presented in two different sections.

2.1. Phase transitions study of the Bi–Sn system

Eight samples of ∼20 mm diameter, ∼3 mm height and weighing ∼2 g were prepared by mixing pure Bi (>99.8%) and Sn (>99.5%). The samples were then put in alumina crucibles and melted in a resistance furnace under an argon atmosphere. The nominal compositions of the samples were Bi$(1-x)$Snx (x = 12.5, 23.5, 36.5, 74.5, 80.1, 84.9, 89.9 and 95.6, wt%). These were confirmed by X-ray Fluorescence (XRF) and Atomic Absorption Spectroscopy (AAS). All samples were homogenized at 120 °C for 60 min and slowly cooled down to the room temperature at a rate less than 2 °C/min.

Samples were studied by Light Optical Microscopy (LOM) and by SEM in a JEOL JSM 6301 F. The SEM is equipped with an INCA Energy 350 EDS analyzer from Oxford Instruments. A backscattered beam with 15 keV is employed. Internal standards are used for the EDS analysis. The experimental uncertainties of the chemical analysis done by EDS are: Bi ±1.2 wt% and Sn ±0.9 wt%.

The Panalytical X'Pert Pro MPD was used for RT-XRD experiments with bulk samples. CuKα or primary monochromated CuKα_1 radiations were used to collect patterns from 5° to 120° (2θ) with steps of 0.01° and counting time of 10 s. The powder HT-XRD was not performed due to problems related with the samples' grinding (the apparatus used only allows powder HT-XRD).

The DTA/DSC measurements were performed on a SETARAM Labsys TG/DTA/DSC in order to establish the transition temperatures. Alumina crucibles were used and measurements were performed under flowing argon atmosphere (approximately 40 cm^3 min^{-1}). Alumina also served as the reference material. Samples weighing between 0.1 and 0.2 g were measured at the heating rates of (in °C/min) 10.0, 5.0 and 2.0–2.5. Transition temperatures were found for "0 °C/min". The temperatures of the invariant phase reactions were taken from the extrapolated temperatures on the onset of heating. The *liquidus* curve temperatures were taken from the peaks on heating.

The global composition and homogeneity of the samples was checked by SEM/EDS, before and after the DTA/DSC experiments.

2.2. Equilibrium study of the Bi–Sn system

Five alloys have been prepared for the equilibrium study. The samples were prepared by mixing pure Bi (>99.9%) and Sn (>99.9%). The nominal compositions of the samples are Bi$(1-x)$Snx (x = 50, 80, 85, 90 and 95, wt%). Samples were analyzed in a SEM from JEOL JSM 6460. The EDS is from Oxford Instruments and it is equipped with an INCA Energy and Wave. The studies were performed in the back-scattered electron mode with 20 keV. Four of the five samples were also studied by DTA/DSC in a Netzsch DTA/DSC 404. For the latter, samples weighing between 0.1 and 0.2 g were introduced into graphite crucibles. Silver was used as a reference material. The measurements were carried out under flowing argon atmosphere (approximately 40 cm^3 min^{-1}).

2.3. Equilibrium study of the Bi–Zn system

The experimental effort was limited to the investigation of the discrepancies concerning the solubility limit of Zn in (Bi) between the theoretical and experimental assessments.

Two alloys were prepared, one with approximately 0.3 wt% Zn and another one with 76.2 wt% Zn. The low Zn content alloy was expected to lie in the single-phase region of the phase diagram, according to the experimental assessment. Nevertheless, according to calculations, it was expected to lie in the two-phase area.

The experimental alloys were melted under an Argon atmosphere in an ERSCEM PV 8920 spill furnace. Samples of approximately 40 g were injected into a copper mould after 20–30 s of stirring.

The low Zn content (approximately 0.3 wt%) alloy was annealed for 336 h at a temperature of 245 °C, just below the eutectic temperature of 254.5 °C. After annealing, the sample was quenched in water and observed by SEM/EDS. The morphology of the sample did not allow the measurement of the composition of the Zn-rich phase. A second alloy was prepared with composition of 23.8 wt% Bi and 76.2 wt% Zn and was therefore cast and annealed at 200 °C for 864 h. This sample was analyzed by SEM/WDS using pure Bi and Zn as standards.

2.4. Phase transitions study of the Bi–Sn–Zn system

Vertical sections for w(Bi) ∼ 10%, w(Zn) ∼ 12%, and w(Sn) ∼ 5%, 13%, 19%, 40%, 59% and 79% were chosen for

this study. The corresponding 29 samples were prepared and annealed like those in Section 2.1. The samples with w(Sn) ∼ 77/81% were re-annealed for more than 180 min at 120 °C, and cooled down at a rate of 0.5 °C/min or quenched into water from 120 °C.

Samples were studied by LOM and by SEM/EDS in the same conditions as those mentioned in Section 2.1. The experimental uncertainties for the chemical analysis obtained by EDS are: Bi ±1.2 wt%, Sn ±0.9 wt% and Zn ±1.1 wt%.

Bulk RT-XRD measurements were performed to identify the present phases. For some samples, powder HT-XRD measurements were also performed, under a vacuum of 10^{-5} mbar or an argon atmosphere. The furnace used is an Anton Parr Chamber applied to the Panalytical X'Pert Pro MPD (details for the XRD data collection are given in Section 2.1).

DTA/DSC measurements were performed on two heat flux instruments with the possibility of determining the latent heat: a TA Instruments SDT 2960 and a SETARAM Labsys TG/DTA/DSC (mentioned in Section 2.1). Alumina crucibles were used and the measurements were performed under flowing argon atmosphere. A graphite plate was sometimes used at the bottom of the crucible in order to improve the removal of the analyzed sample (especially in the case of those samples whose composition fell over the miscibility gap). Alumina (with a similar shape and weight as the measured samples) was used as reference. The samples were polished and cleaned just before being measured in order to improve thermal contact and to avoid spurious or shifted transition peaks due to oxidation. The heating rates mainly used were 20, 10, 5, 2.5 and/or 2.0 °C/min. Unfortunately, the lower heating rates did not allow the detection of transition temperatures (for example, in the case of liquidus surface of the miscibility gap). Consequently, it was impossible to find the transition temperatures at "0 °C/min" by a linear regression. A calibration factor: $C = b_0 + b_1^* T + b_2^* R + b_3^* R^2$ (T — temperature in °C, R – heating rate in °C/min) was evaluated after performing ten calibrations with five different elements (including pure Sn and Zn). Different heating rates (from 2 to 20 °C/min) were also used for determining the coefficients b_0, b_1, b_2 and b_3. The accuracy of all of the given temperatures is ±1 °C. The temperatures of the invariant phase reactions were taken from the extrapolated onset temperatures on heating. The liquidus surface temperatures were taken from the peaks on heating.

After the DTA/DSC measurements, some Bi–Sn–Zn samples were also investigated by SEM/EDS in order to check their compositions.

2.5. Equilibrium study of the Bi–Sn–Zn system

A second set of experiments were carried out in the scope of this study with the aim of reaching states close to the thermodynamic equilibrium and confirming the previous results. Seven samples with nominal compositions (A – Bi35Sn35Zn30, B – Bi20Sn50Zn30, C – Bi10Sn70Zn20, D – Bi18.5Sn45Zn36.5, E – Bi10Sn70Zn20, F – Bi60Sn30Zn10, G – Bi25Sn37.5Zn37.4 and H – Bi25Sn47.6Zn27.4, wt%) were prepared from pure Bi, Sn and Zn (Bi, Sn, Zn > 99.9%, all supplied by Alfa Aesar). The homogeneity of all samples was checked by SEM/EDS (in a JEOL JSM 6460) in the back-scattered electron mode. The microstructure of the samples was, in all cases, found to be reasonably homogeneous in the whole sample volume. Slices of the samples were annealed at two selected temperatures during different intervals of time, before being quenched into cold water. The first set of alloys (A, B and C) was annealed at 100 °C. For a more detailed study and verification of the previously obtained results, a second set of alloys (D, E, F, G and H) was prepared. The annealing temperature for the second set of samples was 120 °C.

SEM/EDS analysis was used to identify the coexisting phases and to measure their compositions (both overall and phase compositions).

Some of the annealed samples were also studied by DTA/DSC (in a Netzsch DTA/DSC 404). The studied samples correspond to compositions that lay in phase regions where the phase *equilibria* were uncertain. The latter measurements were conducted on samples weighing approximately 0.3–0.4 g, which had been sealed under vacuum in quartz crucibles. Gold was used as the reference material. A heating rate of 2.0 °C/min was employed both for calibration and measurement of the prepared samples. The temperatures of the invariant phase reactions were usually taken from the extrapolated onset on heating. The accuracy of all of the given temperatures is ±2 °C.

Table 1
Bi–Sn experimental data from DTA/DSC

w(Sn) (%)	Transition temperatures (°C)	
12.5	138.9[a]	230.1[c]
23.5	138.9[a]	200.9[c]
36.5	139.0[a]	160.5[c]
74.5	138.7[a]	195.7[c]
80.1	138.2[a]	202.8[c]
84.8	138.4[a]	210.5[c]
89.9	138.0[a]	219.3[c]
95.6	188.9[b]	227.0[c]

Final composition was found after AAS and/or XRF and SEM/EDS.
[a] Eutectic temperatures.
[b] *Solidus* temperatures.
[c] *Liquidus* temperatures.

3. Results and discussion

3.1. Bi–Sn system

The DSC/DTA results obtained for the first eight samples can be seen in Table 1. Their comparisons can be made by studying Fig. 1. The invariant temperature measured for the binary eutectic L ↔ (Bi) + (Sn) is 138.6 ± 0.6 °C, which is in agreement with that proposed in [4,6].

For the equilibrium study, the results of five samples studied are summarized in Table 2, along with the experimental uncertainties associated with the EDS work. It has been found that there are no major differences between equilibrated samples annealed at 190, 430, 600, 770, 890 and 950 h (Table 2). Therefore, an annealing time of around 400 h is

Table 2
Bi–Sn experimental data from DTA/DSC and SEM/EDS for samples in equilibrium

Sample	BS 1	BS 2	BS 3	BS 4	BS 5
w(Sn)	50	80	85	90	95
Annealing at 130 °C					
Time (h)	kin. st.[a]	770	600	890	770
SEM/EDS results – composition measurements (wt%)					
w(Sn)	49.4 ± 0.9	78.4 ± 0.5	83.8 ± 1.1	88.0 ± 0.4	93.2 ± 0.2
Sn in (Bi)	0.5 ± 0.2	N/A	N/A	N/A	N/A
Bi in (Sn)	5.8 ± 0.1	N/A	N/A	N/A	5.4 ± 0.3
DSC results (°C)					
Invariant reactions	[b]	138	138	–	–
Solidus	[b]	–	–	186	201
Liquidus	[b]	205	222	220	229

[a] Kinetic study: three samples were annealed for different times (190, 430 and 950 h). Bi content of BCT_A5 (Sn) analyzed by SEM + EDS (5, 6.2 and 5.8 wt%).
[b] Not measured.

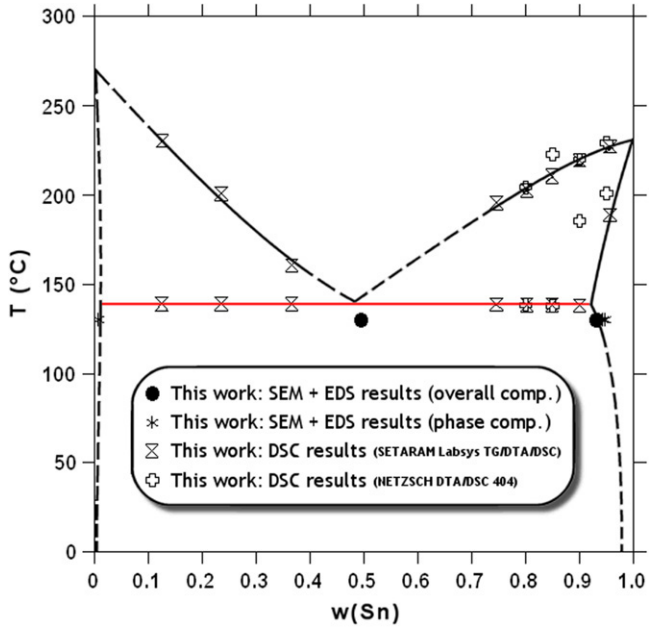

Fig. 1. Bi–Sn experimental phase diagram after results from DTA/DSC and SEM/EDS obtained in the present work. Dashed lines were drawn according to what was expected from our results and having in consideration the literature [6].

sufficient to get close to the equilibrium state. Also, no major discrepancies are found between samples heat treated with annealing times as short as 60 min at 120 °C.

The annealed structures of the samples are elucidated in Fig. 2(a)–(c). They may be viewed as two-phase structures consisting of (Bi) and (Sn), in all of the five alloys annealed at 130 °C. These results are thus consistent with the DTA/DSC results for alloys BS 2 and BS 3 (Table 2).

In disagreement with what was proposed by the authors [6,7], results of this work point to a much lower solubility of Bi in (Sn) (approximately 10 wt% as against approximately 25 wt% [6,7]). On the other hand, the results presented in this paper are apparently in agreement with those proposed by Oelsen and Golücke [5].

The DSC/DTA data obtained with the equilibrated samples, using the Netzsch DTA/DSC 404, point to slightly different solubility of Bi in (Sn) (15 wt%). There are also some discrepancies concerning the Liquid + (Sn) ↔ (Sn). This could be because of the possibility of a slight shift in the corresponding samples' composition.

The authors of the present paper gave more gravity to the data from the set of eight samples (Section 2.1), while assembling the experimental phase diagram. The DTA/DSC data for these eight samples were in agreement with the SEM/EDS and XRD results and also with the results from the ternary Bi–Sn–Zn (Section 3.3).

The microstructure of samples with w(Bi) = 74.5% and w(Sn) = 25.5%, were analyzed by SEM/EDS after being measured by DTA/DSC (and cooled down to room temperature with a rate of 5 °C/min), (Fig. 3). As expected, it confirms the existence of a pro-eutectic and eutectic structure.

The XRD pattern from a bulk sample with w(Bi) = 4.4% and w(Sn) = 95.6%, exhibiting one-phase structure (Sn), is shown in Fig. 4. All other samples from the binary Bi–Sn, detailed in Section 2.1, have been analyzed by RT-XRD. The presence of (Bi) confirms the results of DTA/DSC experiments (Table 1).

3.2. Bi–Zn system

The assessment of Massalski [8] is based on existing experimental results. It indicates a significant solubility of Zn in (Bi) (few wt% of Zn). Nevertheless, the calculations carried out by [9] indicated a much lower solubility (significantly less than 1 wt%). Therefore, the experimental program is focused on the discrepancies of the solubility of the alloying elements in the relevant terminal solid solutions.

The experimental results at 245 °C confirmed the low solubility of Zn in (Bi), as the sample with low Zn content clearly exhibits a two-phase structure (Fig. 5). The results of solubility of both the elements in the respective solid solutions, is shown in Table 3.

3.3. Bi–Sn–Zn system

Muzaffar [3], who thoroughly studied the system by means of thermal arrests, did not measure any point for the *liquidus* surface in the region of the miscibility gap (L1 + L2/Liquid).

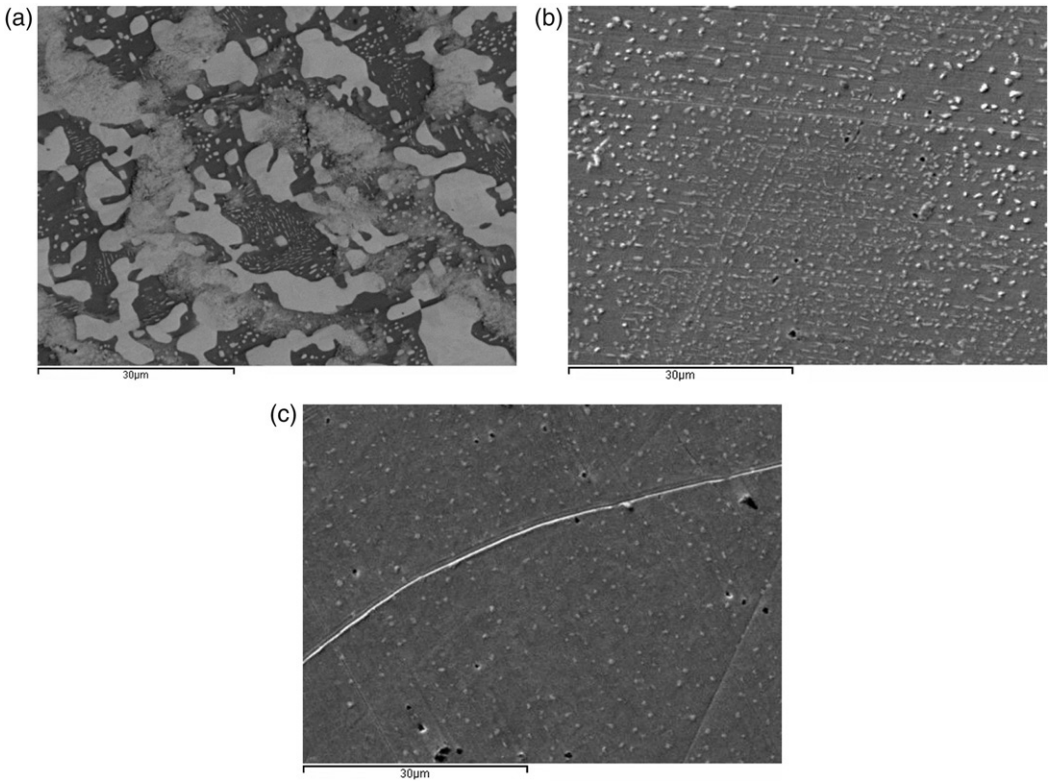

Fig. 2. Microstructure (2000×) of the annealed samples – mixture of light (Bi) and dark (Sn) phases: (a) "BS 1"; (b) "BS 3" and (c) "BS 5".

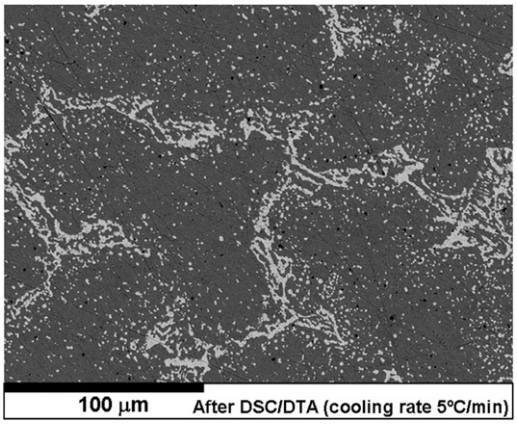

Fig. 3. Microstructure (500×) of the sample with w(Bi) = 74.5% and w(Sn) = 25.5%, after the DTA/DSC experiment with a cooling rate of 5 °C/min: (Bi) – light grey, (Sn) – medium grey.

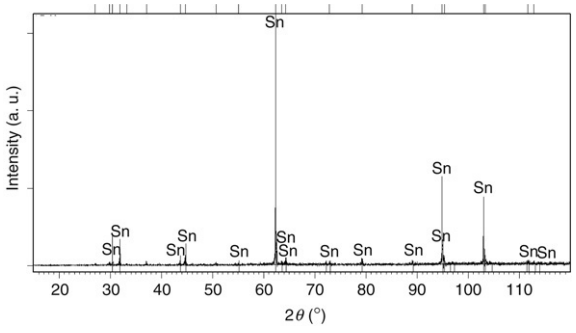

Fig. 4. The XRD pattern at room temperature for a bulk sample with composition: w(Bi) = 4.4% and w(Sn) = 95.6%. This sample was the only one, studied in the Bi–Sn system, which was monophasic (Sn), at room temperature.

Table 3
Composition of the phases present in the Bi–Zn alloy with w(Zn) = 76.2% after the annealing at 200 °C

Phase		Composition of phases (wt%)
(Bi)	Bi	99.7 ± 0.2
	Zn	0.3 ± 0.1
(Zn)	Bi	0.3 ± 0.2
	Zn	99.7 ± 0.2

Fig. 5. Microstructure (1000×) after 336 h of annealing (overall composition: w(Zn) ∼ 0.3 and w(Bi) ∼ 99.7%). The matrix comprises a solid solution of Zn in (Bi) phase and dark particles formed by a solid solution of Bi in (Zn).

In this work, we measured the miscibility gap in the liquid phase by using DTA/DSC at heating rates of 10–20 °C/min.

Table 4
Bi–Sn–Zn experimental data from DTA/DSC and SEM/EDS

Results for Bi–Sn–Zn from DTA/DSC							
w(Bi)	w(Sn) (%)	w(Zn)	Transition temperatures (°C)				
10.0	4.1	85.9	133.7[a]	182.9	394.3	402.5	502.6
20.1	5.0	74.9	133.1[a]	200.6	394.4	406.1	518.2
30.4	5.0	64.6	134.4[a]	217.0	398.7	410.3	524.8
32.8	5.1	62.1	133.7[a]	223.3	405.5	407.5	528.1
43.8	4.7	51.5	133.6[a]	229.4	407.3	413.2	519.8
53.3	4.9	41.8	134.4[a]	230.7	407.1	414.4	509.5
55.4	5.5	39.1	134.2[a]	236.4	409.1	414.0	510.9
68.5	5.7	25.8	133.4[a]	232.9	–	412.1	460.3
31.7	14.3	54.0	133.5[a]	186.0	399.9	401.9	463.0
55.6	13.7	30.7	134.2[a]	212.6	–	403.0	
56.7	12.6	30.7	133.9[a]	217.9	–	404.3	
74.0	11.9	14.1	133.9[a]	223.0	360.3		
11.7	18.0	70.3	134.3[a]	153.7	384.5	393.7	439.4
26.5	18.2	55.3	135.1[a]	138.0	390.7	399.2	443.9
28.0	17.8	54.2	133.5[a]	148.0	394.6	399.0	447.0
37.9	19.8	42.3	134.4[a]	171.4	395.4	404.9	
51.1	21.4	27.5	134.6[a]	177.6	386.7		
55.0	28.9	16.1	134.8[a]	170.4	343.7		
10.1	40.1	49.8	134.0[a]	182.6	367.7		
23.7	38.5	37.8	135.1[a]	161.4	367.0		
47.2	40.4	12.4	134.1[a]	137.7	295.4		
30.6	45.8	23.6	133.4[a]	143.2	341.7		
37.2	44.1	18.7	133.5[a]	147.1	344.9		
10.1	57.8	32.1	134.0[a]	187.2	330.0		
18.2	59.5	22.3	134.2[a]	181.5	299.5		
29.3	58.5	12.2	134.8[a]	165.6	254.7		
4.7	76.5	18.8	–	168.8	193.3	282.2	
9.2	81.0	9.8	131.0	188.2	231.5		
9.6	81.0	9.4	131.7	182.6	230.1		

Average compositions for the solid phases of Bi–Sn–Zn from SEM/EDS (calculated from 29 samples) (for $T < 120$ °C)

Phase	Composition of phases (wt%)		
	$w(Bi)_{av.} \pm 1.2\%$	$w(Sn)_{av.} \pm 0.9\%$	$w(Zn)_{av.} \pm 1.1\%$
(Bi)	95.5	1.9	2.6
(Sn)	4.4	93.3	2.3
(Zn)	0.2	0.3	99.5

Final composition was found after AAS and/or XRF and SEM/EDS.
[a] Eutectic temperatures.

The results, listed in Table 4, are plotted in Figs. 6 and 7. In some cases, the cooling curve is helpful in identifying the peak corresponding to the *liquidus* temperature. It is difficult to find *liquidus* surface' peaks for samples belonging to the vertical section w(Sn) ∼ 5%, with w(Bi) ∼ 20% and 70%; which may be due to the spinodal effect. The *liquidus* temperatures for these two samples are shown in Table 4 but it has to be taken into account that the experimental uncertainty can be higher for these two samples than for the rest. An example of a DTA/DSC curve obtained for a sample with w(Bi) = 53.3%, w(Sn) = 4.9% and w(Zn) = 41.8% is depicted in Fig. 8.

DTA/DSC results from equilibrated samples are in agreement with the previous ones (Table 5).

The invariant temperature measured for the ternary eutectic L ↔ (Bi) + (Sn) + (Zn) is 134.1 °C ± 1.0 °C which is 4.2 °C higher than that proposed in [3].

All samples in Table 4 have been analyzed by bulk XRD at room temperature after being annealed for 60 min at 120 °C and slowly cooled down to room temperature. All peaks were searched/matched using the ICDD PDF-2 2003 database [10–12]. The results show that all samples are homogeneous and that belong to the three-phase region (Bi) + (Sn) + (Zn) (see Fig. 9). Despite the fact that XRD results are in agreement with what was expected from the phase diagrams, the search/match for (Sn) indicated that its reflections are slightly shifted with respect to their position for pure Sn. This maybe due to a

Table 5
Experimental results obtained from Bi–Sn–Zn alloys, annealed at 100 °C

Sample		A	B	C
Composition (wt%)		Bi35–Sn35–Zn	Bi20–Sn50–Zn	Bi10–Sn70–Zn
Annealing at 100 °C				
Time (h)		744	980	980
SEM/EDS results – composition measurements (wt%)				
Overall	Bi	35.5 ± 0.7	22.4 ± 0.4	11.1 ± 0.3
	Sn	33.6 ± 0.9	54.8 ± 0.5	71.9 ± 0.5
	Zn	30.9 ± 0.9	22.8 ± 0.6	17.0 ± 0.6
(Bi)	Bi	95.9 ± 0.8	96.6 ± 0.7	94.4 ± 1.3
	Sn	0.4[a]	0.7 ± 0.4	3.0 ± 1.0
	Zn	3.7 ± 0.6	2.7 ± 0.7	2.6 ± 1.0
(Sn)	Bi	3.6 ± 0.9	4.3 ± 0.3	3.9 ± 0.4
	Sn	93.3 ± 1.0	94.0 ± 0.6	94.6 ± 0.4
	Zn	3.1 ± 1.0	1.7 ± 0.5	1.5 ± 0.3
(Zn)	Bi	0.7 ± 0.2	0.4[a]	0.4[a]
	Sn	0.7 ± 0.3	0.5 ± 0.2	1.5 ± 0.5
	Zn	98.6 ± 0.3	99.5 ± 0.2	98.2 ± 0.7

Sample	D		E[b]	F[b]	G	H
Comp. (wt%)	Bi18.5–Sn45–Zn		Bi10–Sn70–Zn	Bi60–Sn30–Zn	Bi25–Sn37.6–Zn	Bi25–Sn47.6–Zn
Annealing at 120 °C						
Time (h)	1175		1175	1100	1175	1100
SEM/EDS/WDS results – composition measurements (wt%)						
Overall	Bi	19.6 ± 0.5	14.0 ±0.5	61.2 ± 1.1	30.6 ± 1.2	27.3± 1.6
	Sn	48.2 ± 0.7	68.1 ± 1.0	33.9 ± 1.4	40.8 ± 1.1	52.7 ± 1.3
	Zn	32.2 ± 0.9	17.9 ± 1.0	4.9 ± 0.5	28.6 ± 1.4	20.0 ± 1.7
(Bi)	Bi	97.7 ± 0.7		99.2 ± 0.2	97.6 ± 0.5	99.2± 0.2
	Sn	0.6 ± 0.2	N/A	0.4 ± 0.2	0.6 ± 0.2	0.3 ± 0.2
	Zn	1.7 ±0.5		0.4 ± 0.2	1.8 ± 0.5	0.5 ± 0.3
(Sn)	Bi		4.8 ± 0.6	4.4 ± 0.3		
	Sn	N/A	93.5 ± 0.8	94.8 ± 0.6	N/A	N/A
	Zn		1.7 ± 0.7	0.8 ± 0.6		
(Zn)	Bi	0.1[c]	0.0	0.0	0.4 ± 0.5	0.4 ± 0.4
	Sn	0.6 ± 0.3	0.3 ± 0.2	0.3 ± 0.1	0.4 ± 0.3	0.5 ± 0.1
	Zn	99.3 ± 0.3	99.7 ± 0.2	99.7 ± 0.1	99.2 ± 0.7	99.1 ± 0.4
DTA/DSC results (°C)						
Invariant		135	134	136	136	135
Liquidus		364	297	300	376	340
Others		174	193	168	160	168

[a] These values are not reliable because of the accuracy limitations of EDS and/or very small size of (Bi) or (Sn) particles in the structure.
[b] SEM/WDS was used for the analysis of selected phases: for the "E" sample (Sn) and (Zn), and for the "F" sample (Bi) and (Sn) phases were measured (pure Bi, Sn and Zn standards were used).
[c] The values are not reliable because of the accuracy limitations of EDS and/or very small size of (Bi) or (Sn) particles in the structure. N/A – The values of phase compositions could not be reliably measured because of formation of a mixture of tiny (Bi) particles in (Sn) matrix (see Fig. 11).

distortion of the cell by the partial substitution of Sn by Zn and Bi. We could not detect a similar effect for (Bi); this is probably because the solubility of Sn in (Bi) is significantly smaller than the solubility of Bi in (Sn). In addition, the covalent radius of Bi (0.154 nm) [13] is slightly bigger than that of Sn (0.146 nm) [13] possibly increasing this effect.

HT-XRD measurements were performed from 30 to 180 °C with temperature increments of 10 °C. The HT-XRD diffraction patterns can be observed in Fig. 10. The (Sn) peaks (Fig. 9) could not be detected for temperatures higher than 120 °C because the peaks were too small due to the eutectic reaction occurring at 134 °C. An amorphous phase could be detected for higher temperatures (a halo – a curved baseline – is observed for 2θ between 20° and 40°). It corresponds to the liquid phase. As expected, with the increase in the amount of liquid the concavity also increases. Special attention should be given to the behavior of the [002] plane in (Zn) ($T = 30$ °C, $2\theta = 36.37°$; $d = 0.247$ nm) slightly above the ternary eutectic reaction where the inter-atomic distance, d, slightly decreases. This is in contradiction to the expected tendency to increase with temperature probably due to the rearrangement initiated by the appearance of liquid.

Table 4 lists the solubility of each element in all solid solutions measured by SEM/EDS. The temperature is

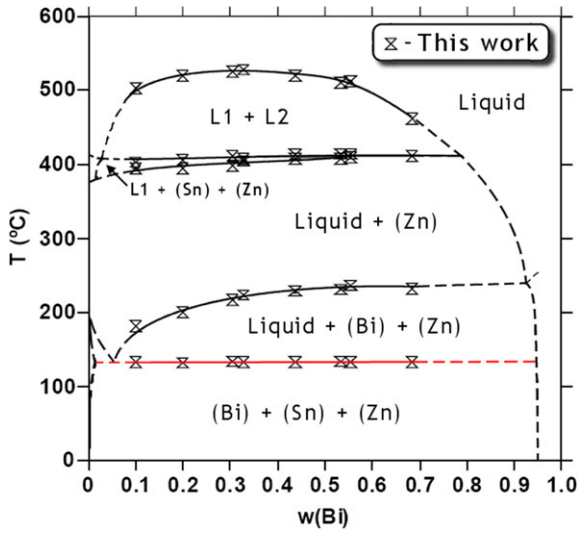

Fig. 6. Experimental vertical section for w(Sn) ∼ 5%. Symbols point for the experimental transition temperatures obtained by DTA/DSC in the present work. Dashed lines were drawn according to what was expected from our results and having in consideration the literature [3].

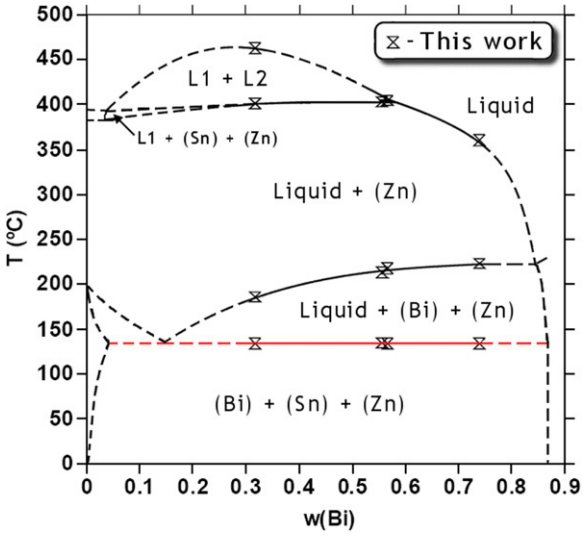

Fig. 7. Experimental vertical section for w(Sn) ∼ 13%. Symbols point for the experimental transition temperatures obtained by DTA/DSC in the present work. Dashed lines were drawn according to what was expected from our results and having in consideration the literature [3].

considered to be less than 120 °C because samples are annealed at 120 °C for 60 min and slowly cooled down to room temperature. Fig. 11 envisages four SEM microstructures of some selected samples showing the three different phases, in accordance with the expectation.

Three samples with w(Sn) ∼ 77/81% have been subjected to two different heat treatments consisting of an annealing at 120 °C for 180 min followed by slow cooling at 0.5 °C/min and an annealing for 180 min at 120 °C, followed by water quenching. Our intention concerning the first heat treatment is to obtain phases' composition near room temperature, comparable with those already referred. For the second heat

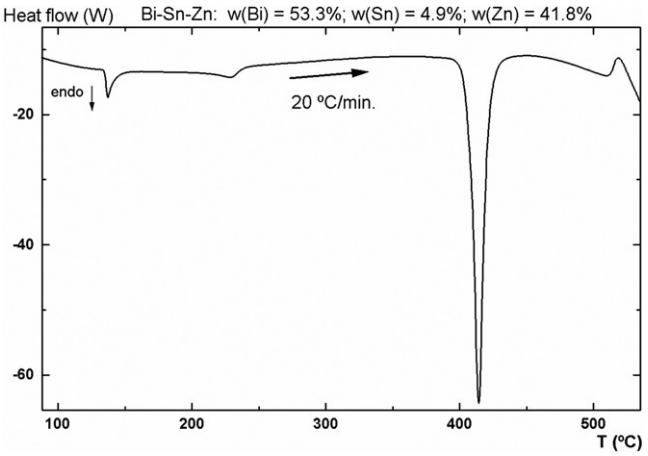

Fig. 8. An example of a DTA/DSC heating curve. The composition of the sample is presented in the figure.

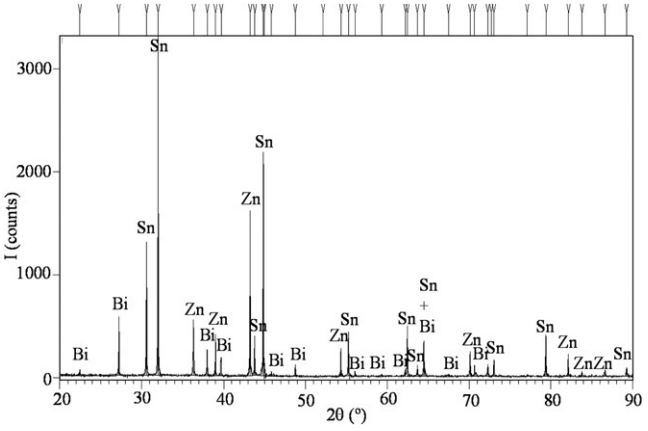

Fig. 9. A XRD pattern at room temperature for a bulk sample with composition: w(Bi) = 10.1%, w(Sn) = 57.8%, w(Zn) = 32.1%.

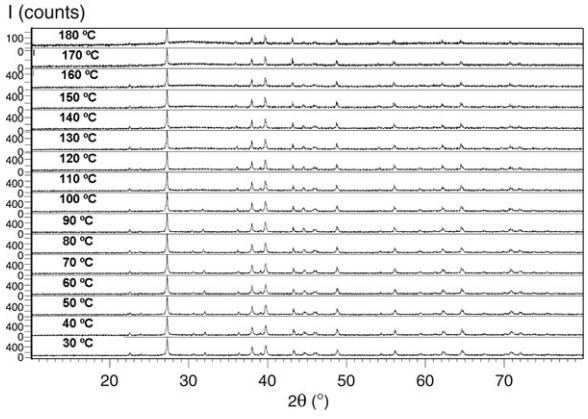

Fig. 10. HT-XRD patterns for a powder sample with composition: w(Bi) = 68.5%, w(Sn) = 5.7%, w(Zn) = 25.8% from room temperature to 180 °C.

treatment, we aim at obtaining the phases' composition at 120 °C. The results show, in both cases, a similarity between phases' composition measured by EDS. This similarity could

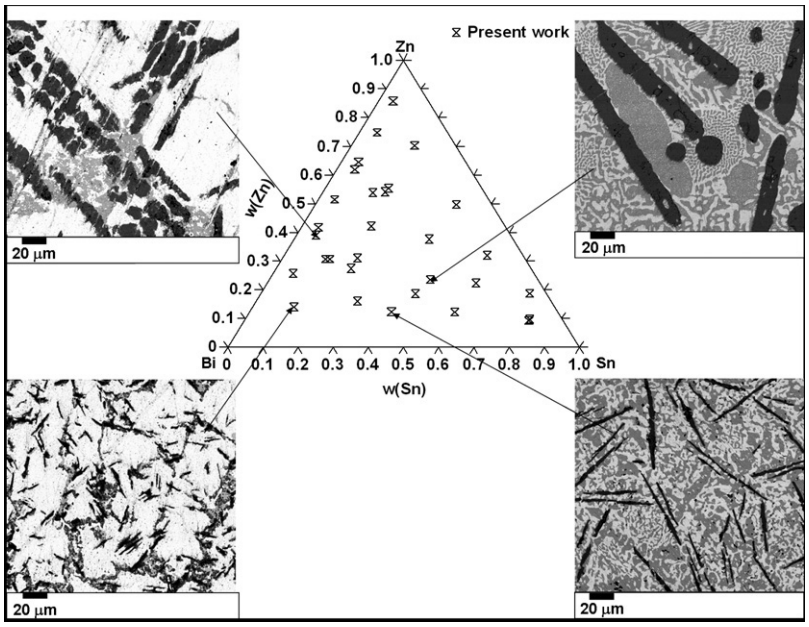

Fig. 11. Microstructures of selected samples (500×): (Bi) – light grey, (Sn) – medium grey, (Zn) – dark grey. The composition of samples is indicated by arrows. All studied Bi–Sn–Zn samples are indicated in the figure.

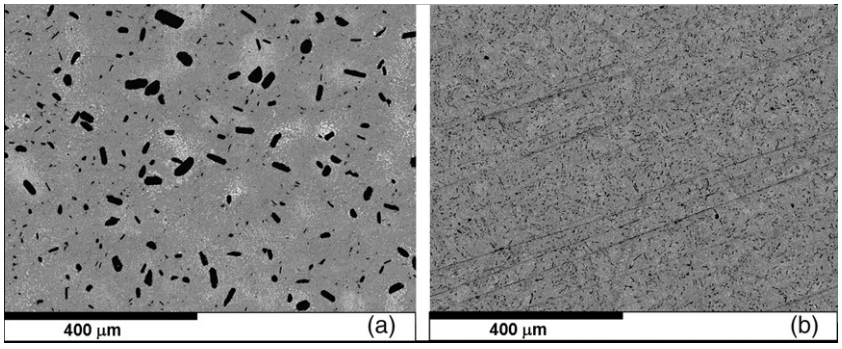

Fig. 12. Microstructures (150×) of a sample with w(Bi) = 9.2%; w(Sn) = 81.0%; w(Zn) = 9.8% after: (a) slow cooling (0.5 °C/min) after 180 min at 120 °C and in (b) water quenched after 180 min at 120 °C: (Bi) – light grey, (Sn) – medium grey, (Zn) – dark grey.

be a result of the short annealing stage, not sufficient to reach the thermodynamic equilibrium. It could also be an effect of the used cooling rate, which is not high enough to "freeze" the "high-temperature" structure. The main difference between samples annealed in different ways reflects in the grain size (Fig. 12).

Concerning the *solvus* of (Bi) and (Sn), SEM/EDS results from samples which previously underwent DTA/DSC experiments, followed by cooling at a rate of 5 °C/min, are also in agreement with the above mentioned results.

As mentioned in Section 2.5, the Bi–Sn–Zn system is also an object of equilibrium study. Examples of the equilibrated samples resulting in microstructures are shown in Figs. 13(a)–(b) and 14(a)–(c).

The results hence obtained agree with the Bi–Sn experimental results (see Section 3.1) and confirm the errors in the predicted phase boundaries. The experimental results also confirmed the observation of Malakhov [9], that the presence of Sn increases the solubility of Zn in (Bi). This increase is significant as the value measured in the ternary alloy is several times higher than the value measured in the binary Bi–Zn system.

Tables 4 and 5 list the results of DTA/DSC measurements (namely the transition temperature found for lower Bi content, corresponding to probable ternary eutectic reaction), which confirmed a much lower Bi solubility in (Sn) than previously anticipated in [6].

4. Conclusions

1. Results from DTA/DSC, SEM/EDS/WDS, RT-XRD and HT-XRD (for some samples) are obtained for the Bi–Sn, Bi–Zn and Bi–Sn–Zn systems and critically compared. New values for the *liquidus* surface of the ternary miscibility gap have also been obtained.
2. Results are generally in agreement with each other. The binaries' results confirm those obtained for the ternary and vice-versa.

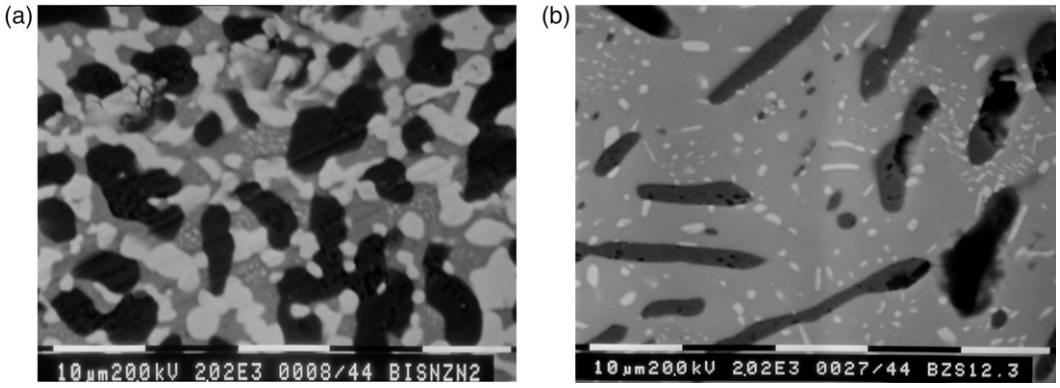

Fig. 13. Microstructure (2000×) of the Bi–Sn–Zn samples (a) "A" (annealed 744 h) and (b) "C" (annealed 980 h), showing a grey matrix of a solid solution of Bi and Zn in (Sn), dark Zn-rich and light Bi-rich phases (both are also solid solutions).

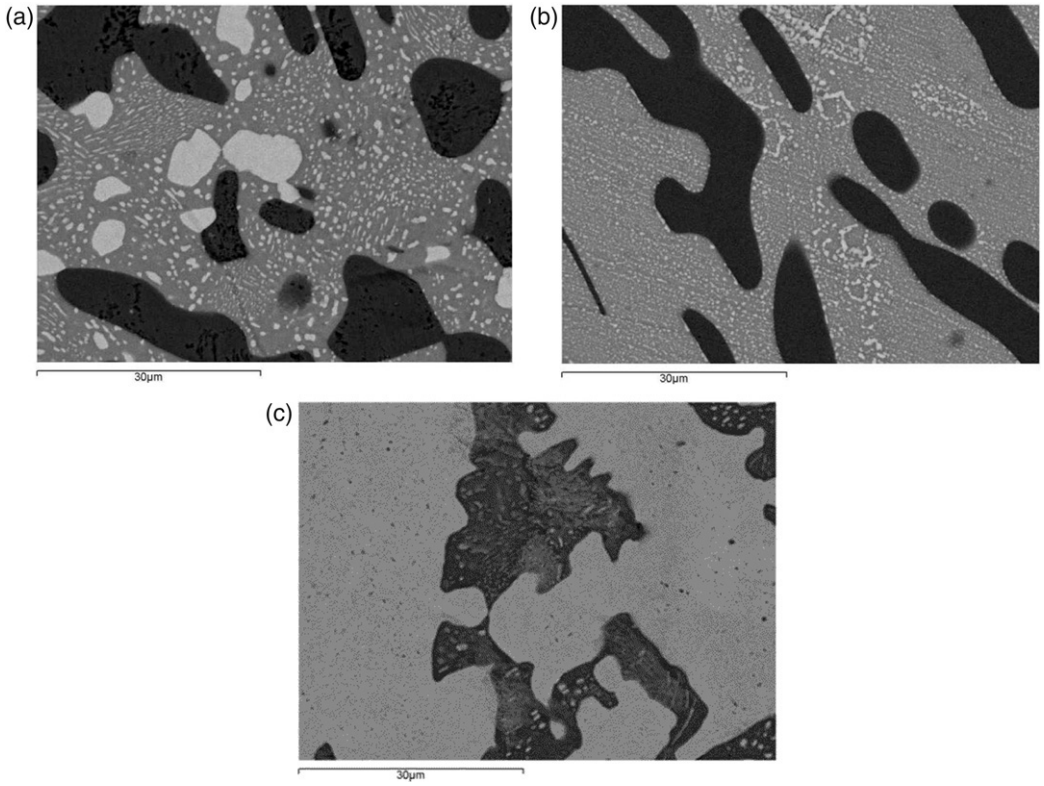

Fig. 14. Microstructure (2000×) of the Bi–Sn–Zn samples (a) "D" (annealed 1175 h), (b) "E" (annealed 1175 h) and (c) "F" (annealed 1100 h), showing the grey matrix of a solid solution of Bi and Zn in BCT_A5 (Sn), dark Zn-rich and light Bi-rich phases (both are also solid solutions).

3. From the ternary and binary results obtained from different techniques, it appears that the solubility of Bi in (Sn) does not surpass w(Bi) ∼ 10%, at the eutectic temperature, which is not in agreement with the assessed phase diagram in [6].
4. Results for Bi–Zn indicate that the solubility of both elements in the respective solid solution is approximately 0.3 wt% at 200 °C as in [9].
5. A reassessment of the Bi–Sn binary and also Bi–Sn–Zn ternary system is desirable. In a recent work of Vizdal et al. [14], the authors of this work reassessed the Bi–Sn and the Bi–Sn–Zn systems based, among others, on the experimental results presented in this study.

Acknowledgments

This work is a contribution to the European COST 531 Action on "Lead-free Solder Materials". J. Vizdal and A. Kroupa would also like to thanks to the Ministry of Education of the Czech Republic and project COST 531.002 for the support.

References

[1] G. Poupon. http://www.sansplomb.org/doc_presentation/pbissue.pdf, 2004.

[2] COST 531 – site. http://www.univie.ac.at/cost531/, 2005.
[3] S.D. Muzaffar, J. Chem. Soc. 123 (1923) 2341–2352.
[4] S. Nagasaki, E. Fujita, J. Japan Inst. Met. 16 (1952) 317–321.
[5] W. Oelsen, K.F. Golücke, Arch. Eisenhüttenwes. 29 (1958) 689–698.
[6] H. Ohtani, K. Ishida, J. Electron. Mater. 23 (1994) 747–755.
[7] B.-J. Lee, C.-S. Oh, J.-H. Shim, J. Electron. Mater. 25 (1996) 983.
[8] T.B. Massalski, Binary Alloy Phase Diagrams, ASM International, Ohio, 1990.
[9] D.V. Malakhov, CALPHAD 24 (2000) 1.
[10] 01-085-1329 ICDD PDF-2 2003; from ICSD using POWD-12++ after P. Cucka, C. S. Barrett, Acta Crystallogr. 15 (1962) 865–872.
[11] 03-065-7657 ICDD PDF-2 2003; from NIST using POWD-12++ after V. T. Deshpande, D. B. Sirdeshmukh, Acta Crystallogr. 14 (1961) 355–356.
[12] 01-087-0713 ICDD PDF-2 2003; from ICSD using POWD-12++ after H. E. Swanson, E. Tatge, Natl. Bur, Stand. (U.S.), circ. 539, 359 (1953) I1.
[13] The Cambridge Crystallographic Data Centre. http://www.ccdc.cam.ac.uk/products/csd/radii/, 2004.
[14] J. Vizdal, M.H. Braga, A. Kroupa, K.W. Richter, D. Soares, L.F. Malheiros, J. Ferreira, The thermodynamic assessment of the Bi–Sn–Zn system, CALPHAD (2007) (in press).